Journal of Nuclear and Particle Physics 2013, 3(4): 100-107
DOI: 10.5923/j.jnpp.20130304.07

Calculations of Excitation Functions of *(n, p)*, *(n,α)* and *(n, 2n)* Reaction Cross-Sections for Stable Isotopes of $^{58,60,61}Ni$ from Reaction Threshold to 20 MeV

S. Yamoah*, M. Asamoah

Ghana Atomic Energy Commission, National Nuclear Research Institute, P.O. Box LG 80, Accra, Ghana

Abstract The excitation functions for *(n, p)*, *(n,α)* and *(n, 2n)* reaction cross-section from reaction threshold to 20 MeV on three nickel isotopes viz; ^{58}Ni, ^{60}Ni and ^{61}Ni were calculated using the EXIFON code version 2.0. The calculations were performed to investigate the development of the effect of shell structure on neutron induced cross sections to understand the mechanisms of the compound nucleus and pre-equilibrium models. The calculations are compared with experimental data (EXFOR data base) as well as with evaluated data files (ENDF/B-VII.1, JEFF-3.1.2, JENDL-4.0). A good agreement is obtained between the calculated and the experimental data as well as the evaluated data. It is concluded that the EXIFON code version 2.0 is suitable for predicting the reaction cross-section for $^{58,60,61}Ni(n,p)$, $^{58,60,61}Ni(n,\alpha)$ and $^{58,60,61}Ni(n,2n)$.

Keywords Excitation function, Cross section, Pre-equilibrium model, Compound nucleus model, Shell structure effect

1. Introduction

Nuclear structural materials must possess a high resistance to mechanical stress, stability to radiation and high temperature, and low neutron absorption. The common nuclear reactor structure materials are stainless steel with Cr, Fe and Ni as main constituents. The main effect of structural material on reactor neutron balance consists in the absorption of neutron through *(n, p)* and *(n,α)* reactions which have thresholds in the range of few MeV.

Precise knowledge of the excitation function and isotopic effects in the *(n, p)*, *(n,α)* and *(n, 2n)* reaction cross-section are very important in nuclear reactor technology. This is because neutron-induced fission reaction is the most important processes that occur in nuclear reactors, accelerator-driven systems and nuclear explosions. Thus, in order to develop concepts of these reactions, it is necessary to have clear knowledge and nuclear data of the reaction cross-sections for nuclear structural materials, fissile actinides and most important fission products in a given energy range. Several authors [1 - 6] have proposed a large number of empirical and semi-empirical formulae with different parameters for cross-section calculations of the reactions *(n, p)*, *(n,α)* and *(n, 2n)* at different neutron energies.

The *(n,α)* reactions cross-section data is of paramount importance from the viewpoint of fusion and advanced fission reactor technology especially for calculations on nuclear transmutation rates, nuclear heating and radiation damage to the materials used in the construction of the core and inner walls of the reactor.

Measurements of excitation curves for the *(n, p)* reaction on chains of isotopes have revealed an interplay of the compound nucleus and the pre-equilibrium mechanisms with the shapes and magnitudes of the excitation functions from the reaction thresholds up to 20 MeV being described by model calculations using a consistent parameter set.

The (*n*, 2*n*) reaction is the dominant reaction channel in the interaction of around 14 MeV neutrons with medium mass and heavy nuclei. Thus, the knowledge of the (*n*, 2*n*) reaction cross-sections is of special importance for fusion reactor technology, especially for materials that may be used as neutron multipliers for tritium breeding or nuclides for which the (*n*, 2*n*) reaction leads to the production of long-lived radioactive nuclei.

Theoretical understanding of nuclear reactions have been further developed and nuclear reaction models refined to the extent that with appropriate parameterization, nuclear models can be used for inter and extrapolation and for consistency checks of experimental cross-section data. EMPIRE II and Talys-1.2 code are recent and versatile reaction model codes for nuclear reaction cross section.

* Corresponding author:
syyamoah@yahoo.co.uk (S. Yamoah)
Published online at http://journal.sapub.org/jnpp

In this paper, we present computed excitation functions of $^{58,60,61}Ni(n,p)$, $^{58,60,61}Ni(n,\alpha)$ and $^{58,60,61}Ni(n,2n)$ reactions from threshold to 20 MeV using the EXIFON code version 2.0 and have compared the results with the existing experimental data (EXFOR data base) [7] as well as with evaluated data files (ENDF/B-VII.1, JEFF-3.1.2, JENDL-4.0) [8, 9, 10].

The main objective of this study is to investigate the nuclear model calculations on the excitation functions with the shell structure effects option which has been implemented in the EXIFON code as the only adjustable parameter to understand the mechanisms of the compound nucleus and pre-equilibrium models over the neutron energy from reaction threshold to 20 MeV.

2. Calculations

The EXIFON code is based on an analytical model for statistical multistep direct and multistep compound reactions (SMD/SMC model) and predicts emission spectra, angular distributions, and activation cross sections including equilibrium, pre-equilibrium, as well as direct (collective and non-collective) processes [11]. The code is restricted to neutrons-, protons-, and α-induced reactions with neutrons, protons, alphas, photons in the outgoing channels. The EXIFON code uniquely describes the emission spectra (a,xb), where $a,b = n, p, \alpha \text{ and } \gamma$ (neutron, proton, alpha and gamma-ray) as well as excitation function (activation cross section) within a purely statistical multistep reaction model [12]. The approach is based on many-body theory (Green's function formalism) [13, 14] and random matrix physics [15]

In the statistical multistep model, the total emission spectrum of the process (*a, xb*) is divided into three main parts,

$$\frac{d\sigma_{a,xb}(E_a)}{dE_b} = \frac{d\sigma_{a,b}^{SMD}(E_a)}{dE_b} + \frac{d\sigma_{a,b}^{SMC}(E_a)}{dE_b} + \frac{d\sigma_{a,xb}^{MPE}(E_a)}{dE_b} \quad (1)$$

The first term on the right hand side of equation (1) represents the statistical multistep direct (SMD) part which contains from single-step up to five-step contributions. Besides particle-hole excitations also collective phonon excitations are considered. The second term represents the statistical multistep compound (SMC) emission which is based on a master equation. Both terms together (SMD+SMC) represents the first-chance emission process [11]. The last term of equation (1) represents the multiple particle emission (MPE) reaction which include the second-chance, third-chance emissions, etc [11].

These terms are summarised below:

The SMD cross section is a sum over *s-step* direct processes given by:

$$\frac{d\sigma_{a,b}^{SMD}(E_a)}{dE_b} = \sum_{s=1} \frac{d\sigma_{a,b}^{s}(E_a)}{dE_b} \quad (2)$$

The SMC cross section has the form:

$$\frac{d\sigma_{a,b}^{SMC}(E_a)}{dE_b} = \sigma_a^{SMC}(E_a) \sum_{N=N_0}^{N'} \frac{\tau_N(E)}{\hbar} \sum_{(\Delta N)} \Gamma_{N,b}^{(\Delta N)}(E,E_b)\uparrow \quad (3)$$

where $\tau_N(E)$ satisfies the time-integrated master equation

$$-\hbar\delta_{NN_0} = \Gamma_{N-2}^{(+)}(E)\downarrow \tau_{N-2}(E) + \Gamma_{N+2}^{(-)}(E)\downarrow \tau_{N+2}(E) - \Gamma_N(E)\tau_N(E) \quad (4)$$

and

$$\Gamma_N^{(\Delta N)}(E)\downarrow = 2\pi \bar{I}_{BB}^2 \rho_N^{(\Delta N)}(E) \quad (5)$$

The multiple particle emission is expressed as:

$$\frac{d\sigma_{a,xb}^{MPE}(E_a)}{dE_b} = \sum_c \frac{d\sigma_{a,cb}(E_a)}{dE_b} + \sum_{c,d} \frac{d\sigma_{a,cdb}(E_a)}{dE_b} + \ldots.. \quad (6)$$

To keep the model tractable, a simple two-body interaction is assumed [11]:

$$I(r_1,r_2) = -4\pi \frac{F_0}{A} [\chi_{nl}(R)]^{-4} \delta(r_1 - r_2)\, \delta(r_1 - R) \quad (7)$$

with $F_0 = 27.5\ MeV$ taken from nuclear structure considerations. The factor $[\chi_{nl}(R)]^{-4}$ contains the wave function at the nuclear radius $R = r_0 A^{1/3}$.

The single-particle state density of particles $c = n, p, \alpha$ with mass μ_c is given by:

$$\rho(E_c) = \frac{4\pi V \mu_c (2\mu_c E_c)^{1/2}}{(2\pi\hbar)} = \left(4.48\times10^{-3}\ fm^{-3}\ MeV^{-3/2}\right) r_0^3 A E_c^{1/2} \quad (8)$$

where $V = \frac{4\pi R^3}{3}$ is the nuclear volume.

The single-particle state density of bound particles (at Fermi energy) is then defined by

$$g = 4\rho(E_F) \quad (9)$$

2.1. Shell Structure Effects

The shell structure effects are considered in SMC processes. Under such a situation, the single-particle state density g, in equation (9) is multiplied by the factor [11]:

$$\left(1+\frac{\delta W}{E_X}\left[1-\exp\left(-\gamma E_X\right)\right]\right) \quad (10)$$

with $\gamma = 0.05 MeV^{-1}$ and δW as the shell correction energy taken from tables [11].

The quantity $E_X = E \text{ or } U$ denotes the excitation energy of the composite or residual systems, respectively.

The calculations in this study was performed *with* ($\delta W \neq 0$) and *without* ($\delta W = 0$) shell corrections.

3. Results and Discussion

The results of the excitation function calculations of $^{58,60,61}Ni(n,p)$, $^{58,60,61}Ni(n,\alpha)$ and $^{58,60,61}Ni(n,2n)$ are plotted in Figs 1-9 together with the experimental data taken from the EXFOR data library and the evaluated data files (ENDF/B-VII.1, JEFF-3.1.2, JENDL-4.0). The formation of the compound nucleus is evidenced by the bell-like shape of the excitation functions as observed in all cases under consideration (Figs 1-9). The bell-like shape of excitation curves is a typical characteristic of compound nucleus formation whose cross-section rises abruptly above the reaction threshold and descends as a result of competitive reactions and the increase of the pre-equilibrium contribution with neutron energy.

The excitation curve for $^{58}Ni(n,p)^{58}Co$, $^{58}Ni(n,\alpha)^{55}Fe$ and $^{58}Ni(n,2n)^{57}Ni$ are shown in Figs 1-3.

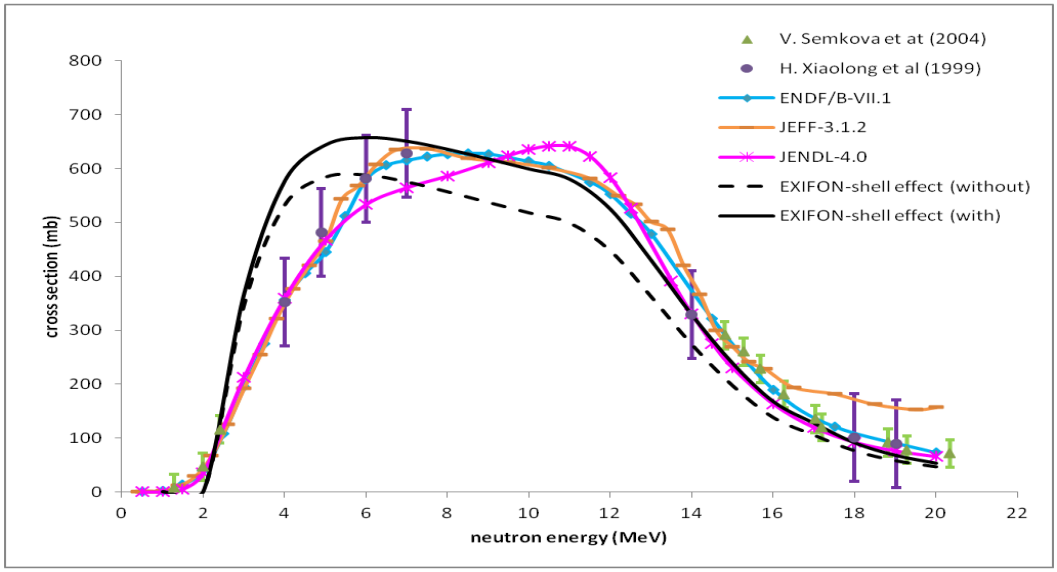

Figure 1. Excitation function for $^{58}Ni(n,p)^{58}Co$ reaction along with experimental and evaluated results. (See above-mentioned references for further information.)

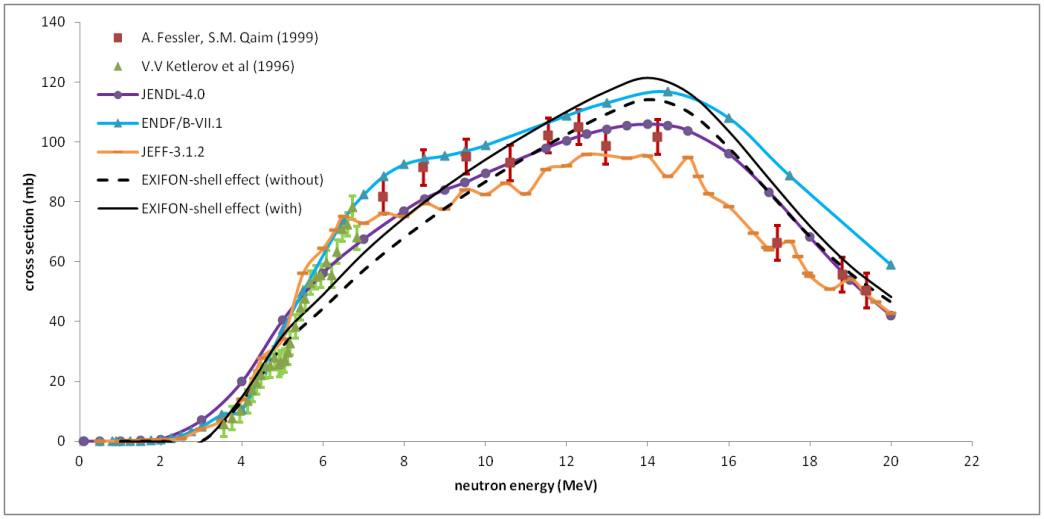

Figure 2. Excitation function for $^{58}Ni(n,\alpha)^{55}Fe$ reaction along with experimental and evaluated results. (See above-mentioned references for further information.)

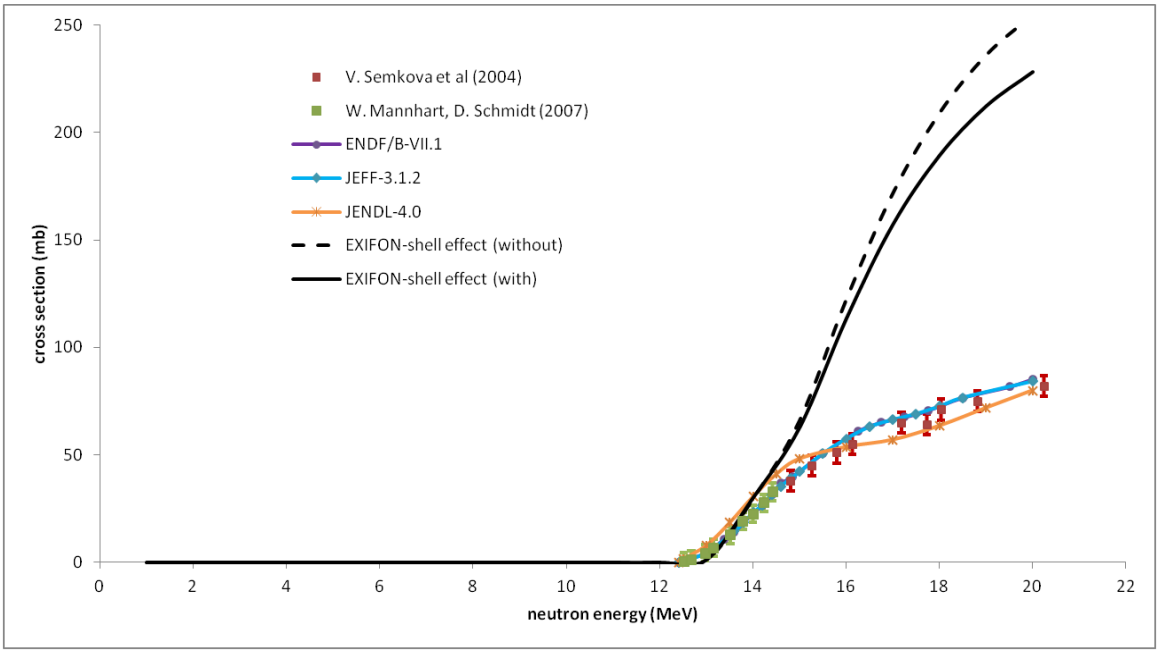

Figure 3. Excitation function for $^{58}Ni(n,2n)^{57}Ni$ reaction along with experimental and evaluated results. (See above-mentioned references for further information.)

As can be observed from Figs. 1-3 the calculations are reasonably in good agreement with the experimental data (EXFOR) as well as the ENDF data files (ENDF/B-VII.1, JEFF-3.1.2, JENDL-4.0). However, for the reaction $^{58}Ni(n,2n)^{57}Ni$, there is much deviation between the calculations (EXIFON) and both the experimental data as well as ENDF data files from neutron energy around 15 MeV.

The results of the excitation functions showing the calculations (EXIFON) compared with the experimental data (EXFOR) as well as the ENDF data files (ENDF/B-VII.1, JEFF-3.1.2, JENDL-4.0) for $^{60}Ni(n,p)^{60}Co$, $^{60}Ni(n,\alpha)^{57}Fe$ and $^{60}Ni(n,2n)^{59}Ni$ are shown in Figs 4-6.

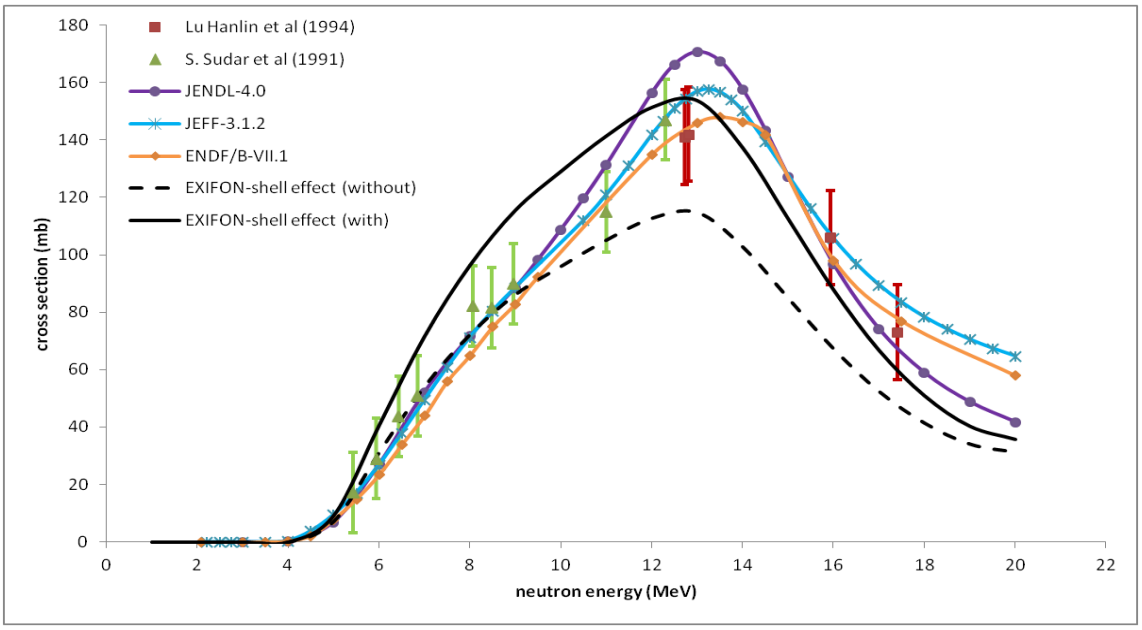

Figure 4. Excitation function for $^{60}Ni(n,p)^{60}Co$ reaction along with experimental and evaluated results. (See above-mentioned references for further information.)

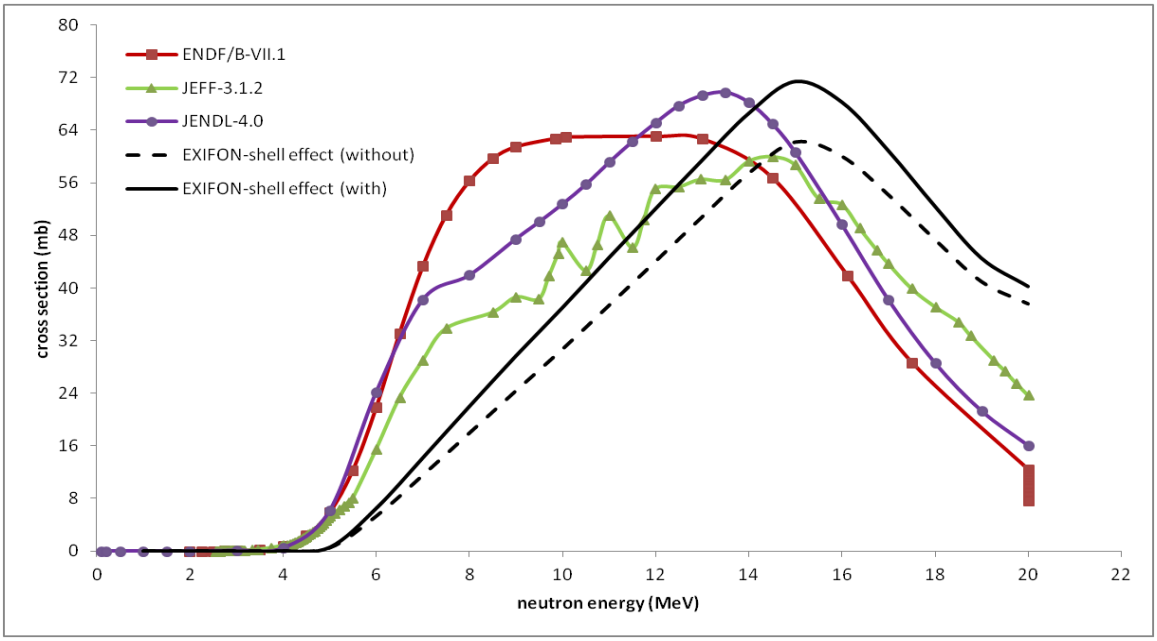

Figure 5. Excitation function for $^{60}Ni(n,\alpha)^{57}Fe$ reaction along with experimental and evaluated results. (See above-mentioned references for further information.)

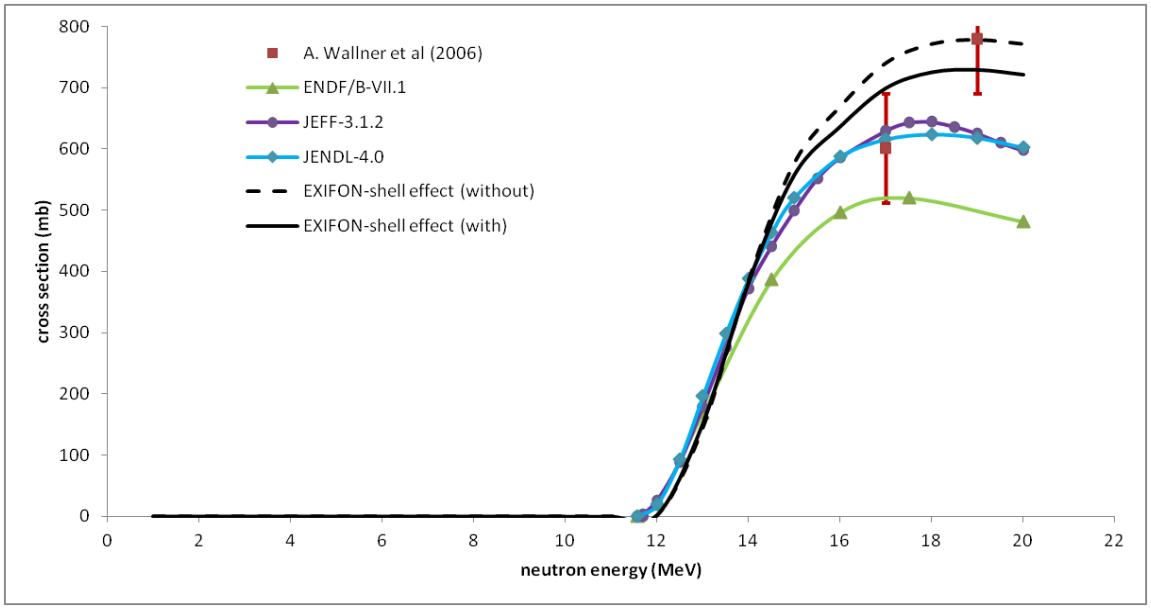

Figure 6. Excitation function for $^{60}Ni(n,2n)^{59}Ni$ reaction along with experimental and evaluated results. (See above-mentioned references for further information.)

As can be observed from Figs 4-6, generally the calculations are in good agreement with the experimental data (EXFOR) as well as the ENDF data files (ENDF/B-VII.1, JEFF-3.1.2, JENDL-4.0). From Fig. 4, at lower neutron energy, the calculations based on shell effect *(without)* predicts the experimental data as well as the ENDF data files much closer than the calculations based on the shell effect *(with)*. At higher neutron energy however, the shell effect *(with)* predicts much closer than the shell effect *(without)*. The opposite is the case in Fig. 5 where at lower neutron energy the shell effect *(with)* is much closer to the ENDF data files and at higher neutron energy, the shell effect *(without)* predicts much closer to the ENDF data files. In Fig. 6 both the experimental data and the ENDF data files are reasonably predicted by both approaches adopted in the code as compared to the case in Fig. 3.

The excitation curve for $^{61}Ni(n,p)^{61}Co$, $^{61}Ni(n,\alpha)^{58}Fe$ and $^{61}Ni(n,2n)^{60}Ni$ are shown in Figs 7-9.

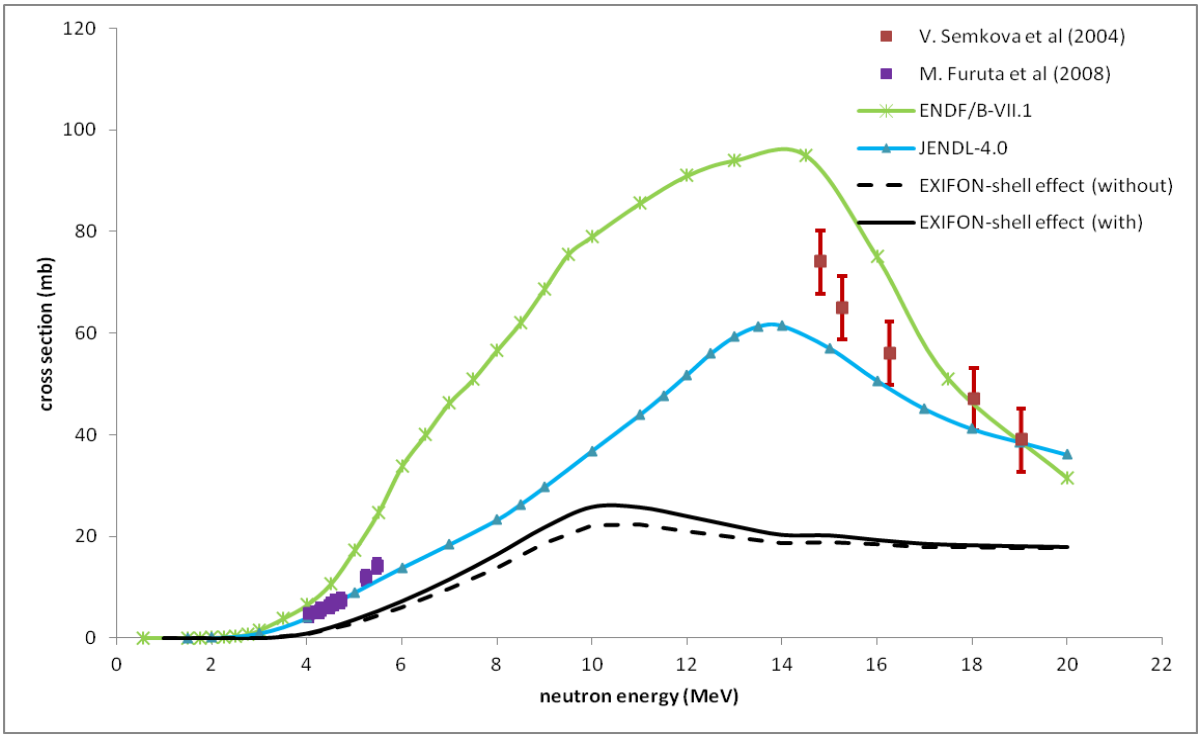

Figure 7. Excitation function for $^{61}Ni(n,p)^{61}Co$ reaction along with experimental and evaluated results. (See above-mentioned references for further information.)

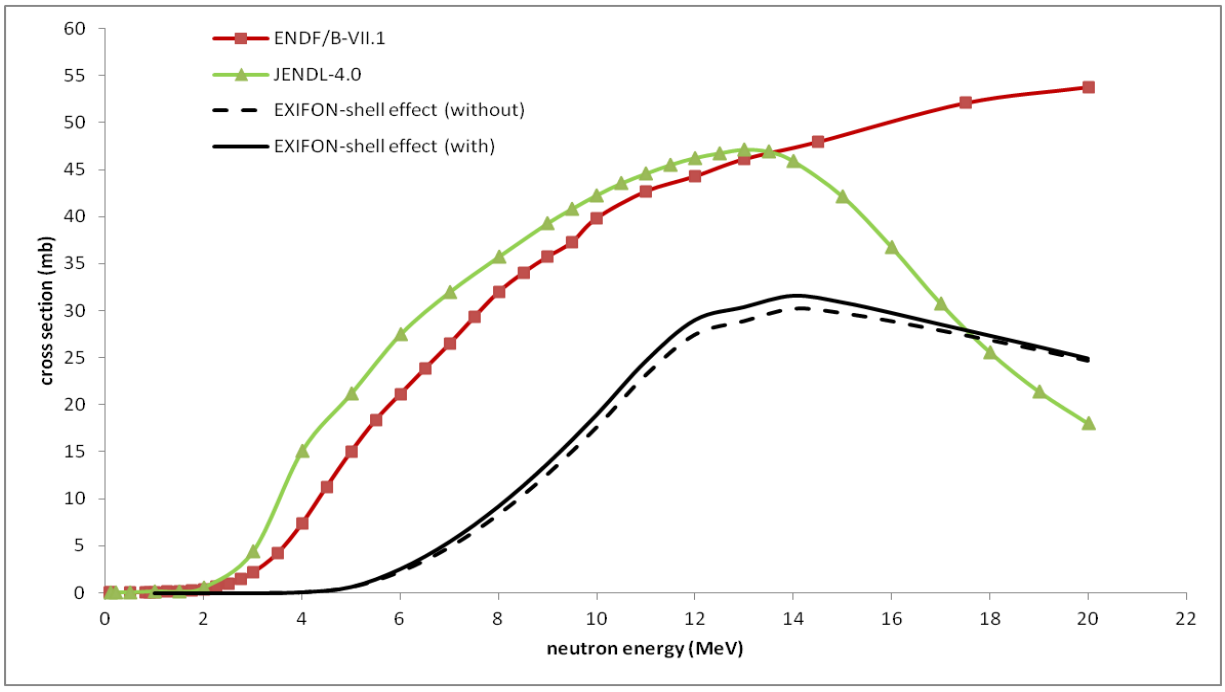

Figure 8. Excitation function for $^{61}Ni(n,\alpha)^{58}Fe$ reaction along with experimental and evaluated results. (See above-mentioned references for further information.)

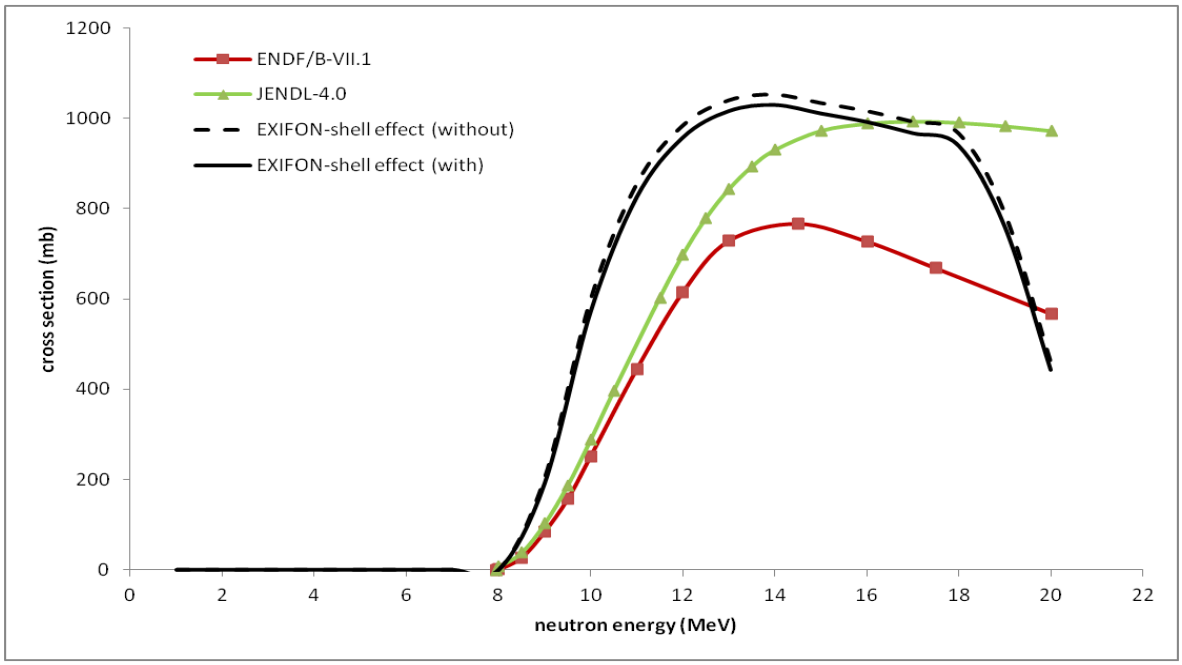

Figure 9. Excitation function for $^{61}Ni(n,2n)^{60}Ni$ reaction along with experimental and evaluated results. (See above-mentioned references for further information.)

Again as can be seen from Figs. 7-9, there is general trend and good agreement between the calculations (EXIFON) and the experimental data (EXFOR) as well as the ENDF data files (ENDF/B-VII.1, JENDL-4.0). It is further observed that there were much deviation between the EXIFON calculations and the experimental and/or ENDF data files. From Figs. 7-8, the calculated cross-sections were much lower that the experimental and/or ENDF data files whereas in Fig. 9 the calculated cross-section were higher than the ENDF data files.

4. Conclusions

The excitation functions of $^{58,60,61}Ni(n,p)$, $^{58,60,61}Ni(n,\alpha)$ and $^{58,60,61}Ni(n,2n)$ reactions from threshold to 20 MeV using the EXIFON code version 2.0 have been performed. The model based calculations of $^{58,60,61}Ni(n,p)$, $^{58,60,61}Ni(n,\alpha)$ and $^{58,60,61}Ni(n,2n)$ reaction cross-sections have been compared with EXFOR experimental data and the ENDF data files (ENDF/B-VII.1, JEFF-3.1.2, JENDL-4.0) and the results are generally in good agreement in all the cases considered under this present study. The bell-like shape of the excitation curves is a typical characteristic of compound nucleus formation with the pre-equilibrium contribution to the total cross-section increasing with mass number. It is concluded that the EXIFON code version 2.0 is suitable in predicting the reaction cross-section for $^{58,60,61}Ni(n,p)$, $^{58,60,61}Ni(n,\alpha)$ and $^{58,60,61}Ni(n,2n)$.

REFERENCES

[1] Habbani F. I., Osman K T., 2001. Systematics for the cross-sections of the reactions (n, p), (n, alpha) and (n, 2n) at 14.5 MeV neutrons., *Appl. Radiat. Isot.* 54(2), 283-290.

[2] Tel E, Sarer B, Okuducu S, Aydin A, Tanir G., 2003. A new empirical formula for 14–15 MeV neutron-induced (n, p) reaction cross sections. *J. Phys. G: Nucl. Part. Phys*. 29, 2169-2177

[3] Tel E, Sarer B, Okuducu S, Aydin A, Tanir G., 2004. The Study of the (n, 2n) Reaction Cross-Sections for Neighbour Deformed Nuclei in the Region of Rare-Earth Elements. *Acta Phys. Slov*. 54(2), 191-204

[4] Kumabe I, Fukuda K. J., 1987. Emprical Formulas for 14-MeV (n,p) and (n,α) Cross Sections *Nucl. Sci. Tech.* 24, 83.

[5] Belgaid M, Tassadit A, Kadem F, Amokrane A., 2005. Semi-empirical systematics of (*n, p*) reaction cross sections at 14.5 MeV neutron energy. *Nucl. Instrum. Methods* B 239(4), 303-313.

[6] Sneh Lata Goyal, Pratibha Gur., 2009: Empirical relation and establishment of shell effects in (*n*, 2*n*) reaction cross-sections at 14 MeV. Pramana J. Phys. 72(2) 355-362.

[7] EXFOR, Experimental Nuclear Reaction Data. <http://www-nds.iaea.org/exfor>.

[8] ENDF/B-VII.1. Evaluated Nuclear Reaction Data. <http://www-nds.iaea.orgendf/>.

[9] JEFF-3.1.2. Joint Evaluated Fission and Fusion file Europe.

<http://www.nea.fr/ dbforms/data/eva/evatapes/jeff_3.1.2/>.

[10] JENDL-4.0. Japanese Evaluated Nuclear Data Library. <http://www.ndc.jaea.go.jp/ jendl/j40/j40.html>.

[11] Kalka H., 1991. EXIFON – *A Statistical Multi-step reaction code*, Report, Technische University Dresden, Germany.

[12] Kalka H, Torjman M, Lien H.N, Lopez R, Seeliger D., 1990. Description of (n-p)- and (n-2n)- Activation Cross Sections for Medium-Mass Nuclei within Statistical Multistep Theory., Z. Phys A – Atomic Nuclei 335,163-171.

[13] Ring P, Schuck P,. 1980. The nuclear many-Body Problem. Springer Verlag, New York

[14] Migdal A. B. 1970. Theory of Finite Fermi Systems and Applications to Nuclei. Wiley Interscience, New York

[15] Brody T. A, Flores J, French J.B, Mello P.A, Pandey A, Wong S.M., 1981. Random matrix physics-spectrum and strength fluctuations., Rev. Mod. Phys. 53, 385-479.